

Porosity Measurement and Densification of Plasma Sprayed Alumina Titania Deposits

K. Murakami

The Institute of Scientific and Industrial Research
Osaka University
8-1 Mihogaoka, Ibaraki, Osaka 567, Japan

C-K. Lin

National Taiwan Ocean University
Keelung 202 Taiwan, R.O.C

S-H. Leigh

Research Institute of Industrial Science and Technology
Materials Research Division, Pohang 790-600, Korea

C. C. Berndt, S. Sampath and H. Herman

Centre for Thermal Spray Research, SUNY at Stony Brook
Stony Brook, New York 11794-2275, U.S.A.

S. Sodeoka

Osaka National Research Institute, AIST
Midorigaoka 1-8-31, Ikeda, Osaka 563, Japan

H. Nakajima

The Institute of Scientific and Industrial Research
Osaka University
8-1 Mihogaoka, Ibaraki, Osaka 567, Japan

Abstract

Al_2O_3 -13 mass% TiO_2 deposits were produced by water-stabilized plasma spraying (WSP). Metastable alumina in the as-sprayed deposit completely decomposed on heat treatment above 1373 K for 8.64×10^4 s. The $\beta\text{-Al}_2\text{TiO}_5$ which formed on heat treatment above the eutectoid temperature of 1553 K induced the formation of cracks (or pores) on cooling. A two stage heat treatment, either above or below the eutectoid temperature, healed cracks and eliminated the detrimental b-phase; thereby resulting in more porosity reduction than prolonged heat treatment

Surface Modification Technologies XI

Edited by T.S. Sudarshan, M. Jeandin and K.A. Khor

© The Institute of Materials, London, 1998

at a higher temperature. A new water Archimedean measurement technique is also proposed which gives more accurate porosity values than the **ASTM** Standard Test Method and the mercury intrusion porosimetry (MIP) technique. An equation is derived for the penetration of water into pores from which pore diameters can be estimated.

1.0 Introduction

Thermal sprayed ceramic deposits generally contain voids such as (i) pores between flattened particles and (ii) vertical cracks arising from the thermal shrinkage of particles during **and/or** after spray processing. In addition to these voids, two types of pores are expected to form in thermal sprayed **Al₂O₃-13mass%TiO₂** deposits. (Note that the terms "pores" or "porosity" are also often used to describe, in a generic sense, the many different types of specific "voids".) It is well known that the rapid cooling of molten alumina or the resulting large undercooling favours the formation of metastable γ -alumina rather than stable **α -alumina**.^{1,2} Unless the substrate temperature is sufficiently high, the major constituent of the as-sprayed deposit is metastable γ -alumina or δ -alumina. Heat treatment can improve the properties of the deposit through the conversion of γ -alumina to **α -alumina** of higher hardness and through a decrease in porosity. They \rightarrow **α** transformation, however, is accompanied by a volume decrease and induces pore formation. When the alumina-titania sintered body is heat treated above the eutectoid temperature of 1553 K, the modulus of rupture of the sintered body is drastically **reduced**.³ This behaviour has been attributed to crack formation on cooling caused by the presence of the high temperature **β -Al₂TiO₅** phase.⁴ The aim of the present work was to study (i) the pore structures and densification of **Al₂O₃-13mass % TiO₂** deposits produced by water stabilized plasma spraying; as well as (ii) phase changes which may occur on heat treatment. A new experimental method and associated data analysis for measuring porosity was also investigated that allowed the above microstructural properties to be examined.

2.0 Experimental Procedure

2.1 Specimen Preparation

A fused-and-crushed powder of **Al₂O₃-13 mass % TiO₂**, Table 1, was thermal sprayed to a thickness of 5 mm onto a 6.4 mm x 51 mm x 152 mm steel substrate using **WSP** equipment (system **PAL160**, The Institute of Plasma Physics, Prague, The Czech Republic). Prior to spraying, the substrate was grit blasted and coated with a thin aluminium layer applied by two wire arc spraying. The **Al₂O₃-13 mass % TiO₂** deposit was separated from the substrate by dissolving the aluminium coating in hydrochloric acid.

2.2 Heat Treatments and Structure Examinations

The deposits were heat treated in air in an electric furnace followed by cooling at **2.78×10^{-2} K/s** (100 K/h). X-ray diffraction patterns were taken of these deposits. The deposits were impregnated with chromium oxide (see **Hamano et al.**⁵ for details) to clearly resolve the pores. The deposits were held above a saturated aqueous solution of chromium trioxide in a vessel at 3.3 **kPa** for 600 s. The deposits were placed into the solution and air introduced into the vessel. Then, the vessel was pressurized to 810 **kPa**, thus forcing the aqueous solution into the **pores**. **These** deposits were dried and heated at 773 **K** for **7.2×10^3 s** (2 h) to convert **CrO₃** to **Cr₂O₃**. This procedure was repeated five times to fill the

Table 1. Constituents of the Feedstock and the Deposits

Specimen	Heat Treatment	γ	δ	α	R	β
Powder	Powder	(γ)	δ	α	R	β
AS	As-sprayed		δ	α	R	β
F11	1173 K x 24 h	γ	δ	α	R	β
F13	1373 K x 24 h			α	R	β
F15	1573 K x 24 h			α	R	β
F17	1723 K x 24 h			α	R	β
F17W	1723 K x 24 h			α	R	β
F17 + 13	+ 1373K x 24h			α	R	

α = α -Alumina, β = β -Al₂TiO₃, γ = γ -Alumina, δ = δ -Alumina and R = Rutile.

The Main Constituent is identified within the shaded boxes.

Brackets indicate a minor component.

pores with Cr₂O₃. Back scattered electron images of the cross sections of these deposits were examined.

2.3 Porosity Measurements

The porosity of the deposits was measured by conventional mercury intrusion porosimetry (MIP) and water Archimedeian methods (WAM). As well, three other test protocols were employed for the WAM. In the first method, the ASTM Standard Test Method (C373-72) was adopted, in which the deposits were boiled in distilled water for 1.8×10^4 s (5 h), followed by soaking for an additional 8.64×10^4 s (1 day). The second method is referred to as a "modified ASTM method" where the deposits were held for 600 s in a desiccator at a pressure of 3.3 kPa above the deaerated distilled water of ambient temperature, and the deposits were placed into the water. Then, the deposits were boiled for 1.8×10^4 s (5 h) at atmospheric pressure, followed by soaking for an additional 8.64×10^4 s (1 day). In the third method, the deposits were immersed in distilled water at 291 K and atmospheric pressure, then the porosity was measured every day by weighing the deposits in water and in air.

3.0 Results

3.1 Phase Composition of the Deposits

Table 1 summarizes the constituents of the as-sprayed and the heat treated deposits. As is well known, the as-sprayed deposit is composed primarily of metastable γ -alumina. Heat treatment at 1173 K converts the main constituent to metastable δ -alumina. In the deposits heat treated at and above 1373 K, the constituents are the phases which appear in the equilibrium phase diagram of the Al₂O₃-TiO₂ system.⁶

The equilibrium eutectoid temperature of the $\text{Al}_2\text{O}_3\text{-TiO}_2$ system has been reported to be 1553 K by Kato et al.³ The $\beta\text{-Al}_2\text{TiO}_5$ detected in deposits F15, F17 and **F17W** at room temperature evolved from incomplete phase decomposition during cooling from above the eutectoid temperature. The absence of $\beta\text{-Al}_2\text{TiO}_5$ in deposit F13 implied that $\beta\text{-Al}_2\text{TiO}_5$ in the as-sprayed deposit (i.e., specimen "AS") was inherited from the feedstock. This speculation is supported by the fact that unmelted powder particles were present in the AS deposit.

3.2 Pore Microstructures of the Deposits

The average thickness of the flattened particles within the deposit was about 9 μm with most splats between 2 μm to 13 μm . The backscattered electron images of the cross-sections of the Cr_2O_3 -impregnated deposits are shown in Figure 1. Pores, including splats which did not appear to be in contact, and vertical cracks were filled with Cr_2O_3 and appeared as white lines. Many pores were interconnected in deposits as-sprayed and heat treated below 1373 K (i.e., Figure 1(c)). As the heat treatment temperature became high, the network structure of the pores was imperceptible and only large pores were seen. This change was most noticeable between 1373 K and 1573 K; i.e., Figures 1(c) and (d).

The surface pores of the deposit, which were subjected to **MIP** and then heated in vacuum to remove the mercury, were filled with petroleum jelly and the volume V of the deposit measured by WAM. The open porosity ε_p (%) of the deposit was calculated from the following equation:

$$\varepsilon_p = \frac{Wv_p}{V} \times 100\% \quad (1)$$

where W is the weight of the deposit without the surface sealing and v_p is the volume of mercury intruded into the deposit of unit weight measured by **MIP**. The result is shown in Figure 2.

Immediately after immersing the deposits in water at atmospheric pressure, numerous small air bubbles appeared from inside the deposits and indicated that pores were connected and that water penetrated into the deposits. The "measured porosity" gradually increased with the soaking time. Even after soaking for 6.05×10^5 (s) (7 days), the "measured porosity" continued to increase. Figure 2 shows the "measured porosity" obtained after 7 days of soaking, together with the porosity measured by other methods.

The porosity measurement of a given deposit increased according to the following order of the particular test method; (i) 7 days soaking, (ii) the conventional ASTM method, and (iii) the modified ASTM method. The open porosity measured by **MIP** was lower than the value found by the modified ASTM method, except for deposit **F11**. Although the difference in porosity between the modified ASTM method and the ASTM method was small when the porosity was high, it became large with decreasing porosity; the ratio being about 1.5 for the **F17+13** deposit.

The porosity increased when the as-sprayed deposit was heat treated at 1373 K or 1573 K. This increase resulted from crack formation due to the volume shrinkage arising from the decomposition of low density γ -alumina to high density α -alumina.² Doubling the heat treatment time at 1723 K does not alter significantly the porosity; whereas heat treatment at 1373 K subsequent to one at 1723 K markedly densified the deposit. The **MIP** results indicated two distinct pore diameters at ~ 0.1 μm and 1 μm (see Figure 3); except for deposit **F11** which was subjected to a less intense heat treatment schedule such that any phase transformations to a stable structure were incomplete. The 0.1 μm pores appear in the deposits which were heat treated above the eutectoid temperature.

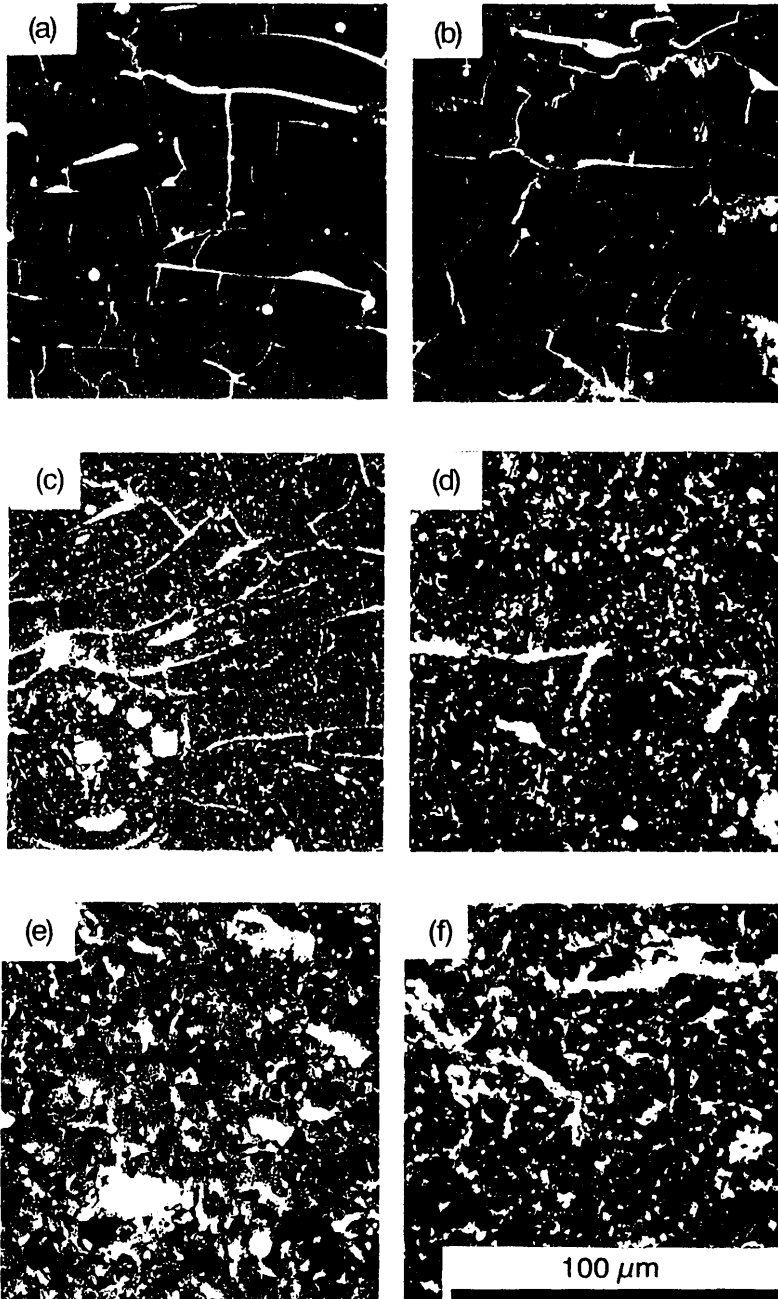


Figure 1: Back scattered electron images of the cross sections of the Cr_2O_3 -impregnated deposits. Heat treatment conditions are: (a) as-sprayed, (b) 1173 K x 24 h, (c) 1373K x 24 h, (d) 1573 K x 24 h, (e) 1723 K x 24 h, and (f) 1723 K x 24 h + 1373 K x 24 h.

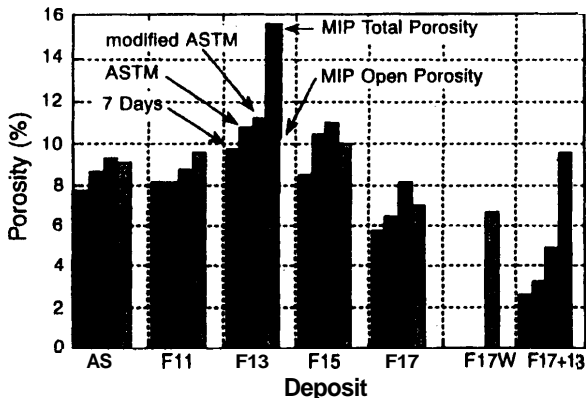


Figure 2: Porosity of the deposits measured by various methods. Heat treatment conditions are: AS = as-sprayed, F11 = 1173 K x 24 h, F13 = 1373 K x 24 h, F15 = 1573 K x 24 h, F17 = 1723 K x 24 h, and F17 + 13 = 1723 K x 24 h + 1373 K x 24 h.

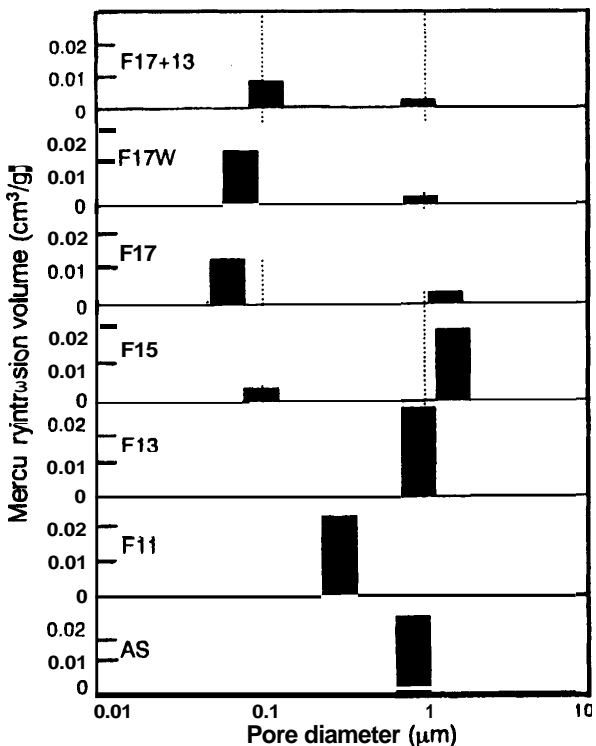


Figure 3: Pore diameter of the deposits measured by the mercury intrusion porosimetry. Heat treatment conditions are: AS = as-sprayed, F11 = 1173 K x 24 h, F13 = 1373 K x 24 h, F15 = 1573 K x 24 h, F17 = 1723 K x 24 h, and F17 + 13 = 1723 K x 24 h + 1373 K x 24 h.

4.0 Discussion

4.1 Porosity Formation and Modification Mechanisms

It is interesting to note that while the porosity was not reduced much by increasing the heat treatment time from 8.64×10^4 s (24 h) to 1.728×10^5 s (48 h) at 1723 K, it decreased significantly after heat treatment at 1723 K for 8.64×10^4 s (24 h) followed by treatment at 1373 K for 8.64×10^4 s (24 h). This result can be explained in terms of crack formation on cooling from above the eutectoid temperature. The densities of α -alumina, rutile and β - Al_2TiO_5 at the eutectoid temperature of 1553 K are estimated from their densities at room temperature⁷⁻⁹ and their thermal expansion coefficients^{10,11}; and are 3.84×10^3 (kg/m³), 4.12×10^3 (kg/m³) and 3.56×10^3 (kg/m³), respectively. Assuming no change in the apparent volume of the deposit, about 3.1% porosity was formed due to phase transformation. Although the volume thermal expansion of β - Al_2TiO_5 is not too different from that of α -alumina and rutile, β - Al_2TiO_5 has a significant expansion anisotropy,¹⁰ which may also form cracks.^{4,10} Thus, the above two mechanisms of crack formation operate.

When deposits containing these new voids were held at 1373 K, which is below the transformation temperature but high enough for the cracks or pores to heal, then porosity would be reduced. The two stage heat treatment proposed in the present work was, thus, more effective in reducing the porosity than the prolonged heat treatment at a high temperature for two reasons: (i) the reduction of porosity through the healing of cracks or pores, and (ii) the elimination of β - Al_2TiO_5 .

4.2 The Modified ASTM Method for Measuring Density

After immersing the deposits in water of 291 K at atmospheric pressure, water gradually penetrated into the deposits and the "measured" porosity increased with soaking time. It is expected that analysis of this time dependency of the measured porosity will provide information on the pore structure; as detailed below.

The water entering the pore channel formed a concave meniscus at the advancing front. Assuming the pore channels to have constant circular cross-sections, the capillary pressure arising from the surface tension of the water is 0.145 MPa and 1.45 MPa when the radii of the channels would be 1 μm and 0.1 μm , respectively. This high pressure would enhance displacement (by the water) of any air remaining in the pore. This air would diffuse out of the deposit down the concentration gradient in the channel. The soaking time dependence of the measured porosity is expressed as follows with the additional assumption that the air diffused under a quasi-steady state; i.e.,

$$E^2 - E_i^2 = 2 \left(\frac{E_0}{L_0} \right)^2 \frac{D(C^* - C_0)RT}{P_0 + \Delta P} (t - t_i) \quad (2)$$

where:

E : the porosity measurement at any time

E_0 : real open porosity

E_i : porosity measured at a specific time $t = t_i$

$L_0 = \tau \xi$; where

τ : tortuosity factor of the pore channel

ξ : half thickness of the deposit

D : 2.3×10^{-9} (m²s⁻¹), the diffusion coefficient of "air" in the water

R : 8.3145 (JK⁻¹mol⁻¹), gas constant

T : 291 (K), temperature

210 Surface Modification Technologies XI

- P_0 : 101.3 (kPa), the atmospheric pressure
 ΔP = $2\sigma\cos\theta/r$ = the capillary pressure at the meniscus; where
 σ : 7.305×10^{-2} (Pa) is the surface tension of water at 291 (K)
 θ : $10\pi/180$ (rad), the contact angle of the water with alumina
 r : the radius of the pore channel
 C^* = $(6.588 \times 10^{-14})(P_0 + \Delta P)^2$ (in mol $\text{kg}_{\text{H}_2\text{O}}^{-1}$)¹²,
 = concentration of air in the water at the meniscus
 C_0 = $(6.588 \times 10^{-14})P_0^2$ (mol $\text{kg}_{\text{H}_2\text{O}}^{-1}$)¹²,
 = concentration of air in the water surrounding the deposit.

Contrary to the case of MIP, the water in the Archimedean method first fills the pore channels with the smallest diameter (since the capillary pressure will be higher for smaller channels) and then proceeds to larger channels. Fifty-six percent of the open porosity in the AS deposit was filled with water after one day of soaking. The position of the water meniscus at this time should correspond to that of the meniscus of the mercury whose intrusion volume equals forty-four percent of the open pore volume. The pore diameter at the latter position is $0.84 \mu\text{m}$ as obtained from the curve of the cumulative mercury intrusion volume vs. pore diameter. The channel diameters (d_{MIP}) can be obtained for the other deposits, Table 2. With a tortuosity factor of six, the channel diameter (d_{WAM}) calculated from eq.(2) fits d_{MIP} for the deposits AS, F11, F13 and F15.

Based on the observation of the fluid flow through unconsolidated porous media, it has been shown¹³ that the tortuosity factor τ ($= L_g/L_e$) has a value of $\sqrt{2}$, where L_g is the geometrical length of the porous medium in the direction of macroscopic flow and L_e is the average effective length of fluid flow in the medium. In the present work, however, the experimental data for deposits AS, F11, F13 and F15 can be explained by taking a tortuosity factor of six. The physical inference is that the pore channels in these four deposits are more tortuous than the flow channels in unconsolidated media. For deposits F17 and F17+13, tortuosity factors from 20 to 40 are necessary for d_{WAM} to be equal to d_{MIP} . These tortuosity factors are large and seem unrealistic. One highly likely explanation is that the pores in these two deposits may be changed to the extreme case of "ink bottle shaped" morphologies as Figure 1 shows. In such a case, the MIP measurement calculates the diameter of the mouth as the pore diameter.

Although eq.(2) predicts a linear relationship between $(E^2 - E_i^2)$ and $(t - t_i)$, the increase in measured porosity became smaller with respect to soaking time than the rate predicted by eq.(2). The pore channels are likely to be interconnected; therefore the meniscus in any pore channel will have the same curvature at a given time. As the water penetrates into the deposit, the curvature becomes larger and the driving force for air dissolution decreases, resulting in a decrease in the penetration rate.

In the modified ASTM method, more than 96 percent of the air in the pores was evacuated before dropping the deposits into the water. Because deaerated water was used, little air will be liberated from the water in the pores during the subsequent boiling. As a result, the modified ASTM method (WAM) provided the larger and more accurate open porosity measurement than the ASTM method.

While the water enters pores spontaneously in the modified ASTM method because water wets alumina, the large contact angle of mercury to alumina requires very high pressures for it to intrude into small pores. Hence, the porosity measured by the former method was higher, except for deposit F11, than that porosity measured by MIP, Figure 2.

4.3 Porosity Components Within a Deposit

The total porosity ϵ_T (%) and the closed porosity ϵ_c (%) of the deposit can be calculated from eqs (3) and (4) when the true density ρ of the material is known.

Table 2. Pore Diameter (in,µm) at the Position of the Water Meniscus After One Day's Soaking

Specimen	D _{WAM}	D _{MIP}
F17 + 13	8.0	0.1
F17	0.6	0.08
F15	0.6	1.2
F13	1.0	0.9
F11	0.5	0.4
AS	1.2	0.8

d_{WAM} is the diameter obtained from water archimedean method and d_{MIP} is the diameter obtained from MIP?

$$\epsilon_T = \left(1 - \frac{W}{\rho V}\right) \times 100\% \tag{3}$$

$$\epsilon_c = \epsilon_T - \epsilon_p (\%) \tag{4}$$

The constituents of the deposits F13 and F17+13 were the stable phases of a-alumina and rutile. Roy and Coble¹⁴ have shown that there was little solubility of TiO₂ in a-alumina when Al₂O₃-TiO₂ specimens were heat treated in air. Assuming that the density of rutile in the deposits F13 and F17+13 is equal to that of pure rutile, the true density of the deposits can be calculated from the densities of a-alumina (3.97 x 10³ kg/m³)⁷ and rutile (4.26 x 10³ kg/m³)⁸ and the chemical composition of the deposits, and is 4.02 x 10³ kg/m³. The calculated closed porosity is shown in Figure 2 for the two deposits. It is seen that the total porosity was from 1.5 to 2.5 times larger than the open porosity. Researchers should, thus, use caution when examining the material properties of thermal spray deposits since the total porosity should be taken into account.

5.0 Conclusions

Al₂O₃-13 mass% TiO₂ deposits were produced by water stabilized plasma spraying, and the pore structures and densification examined with respect to the phase changes brought about by heat treatment. The results are summarized as follows:

1. The metastable alumina phases in the as-sprayed deposit completely decompose to stable phases of a-alumina and rutile when heat treated at 1373 K. The deposits heat treated above the eutectoid temperature of 1553 K contains β-Al₂TiO₅ at room temperature.
2. Two types of pores exist with characteristic diameters of ~ 0.1 µm and 1 µm. The 0.1 µm pores appear in deposits which were heat treated above the eutectoid temperature.
3. Heat treatment above 1573 K alters the pore shape from a relatively simple geometry to an "ink bottle shaped" morphology.

4. A two stage heat treatment, either above or below the eutectoid temperature, is recommended for the purpose of reducing the porosity more effectively than the prolonged treatment at a higher temperature.
5. A new water Archimedean method (WAM) is proposed for the measurement of porosity. The method gives more accurate porosity values than the current ASTM Standard Test Method and mercury intrusion porosimetry.
6. An equation is derived for the penetration of water into the pore channels and this can be used to estimate the channel diameters.

6.0 Acknowledgments

The authors thank Dr. Y. **Makino** (Osaka University) for useful discussions and Dr. R.V. Gansert (formerly of USB) for sample preparation. This work was partially supported by the National Science Foundation under the **STRATMAN** Program DDM 9215846 and MRSEC Program DMR 9632570.

7.0 References

1. R. **McPHERSON**: Formation of Metastable Phases in Flame- and Plasma-Prepared Alumina, *Journal of Materials Science*, 8, 1973, 851.
2. N.N. **AULT**: Characteristics of Refractory Oxide Coatings Produced by Flame-Spraying, *Journal of the American Ceramic Society*, 40(3), 1957, 69.
3. E. **KATO**, K. **DAIMON** and J. **TAKAHASHI**: Decomposition Temperature of β - Al_2TiO_5 , *Journal of the American Ceramic Society*, 63, 1980, 355.
4. J.J. **RASMUSSEN**, G.B. **STRINGFELLOW**, I.B. **CUTLER** and S.D. **BROWN**, Effect of Impurities on the Strength of Polycrystalline Magnesia and Alumina, *Journal of the American Ceramic Society*, 48, 1965, 146.
5. Y. **HAMANO**, J.I. **MUELLER** and R.C. **BRADT**: Chromic Acid Impregnation Strengthening of Porous Alumina, *Ceramic International*, 15, 1989, 7.
6. Phase Diagram for Ceramists, 1975 Supplement, E.M. **Levin** and H.F. **McMurdie**, eds. The American Ceramic Society, Inc., OH, 1975, 135.
7. *CRC Handbook of Chemistry and Physics*, 67th edn., R.C. Weast ed. CRC Press, Inc, Boca Raton, Florida, 1986-1987, B-68.
8. *CRC Handbook of Chemistry and Physics*, 67th edn, R.C. Weast ed, CRC Press, Inc, Boca Raton, Florida, 1986-1987, B-140.
9. C.E. **HOLCOMBE**, Jr. and A.L. **COFFEY**, Jr.: Calculated X-ray Powder Diffraction Data for Beta Al_2TiO_5 , *Journal of the American Ceramic Society*, 56, 1973, 220.
10. G. **BAYER**: Thermal Expansion Characteristics and Stability of Pseudo Brookite-Type Compounds, Me_3O_5 , *Journal of Less Common Metals*, 24, 1971, 129.
11. *Thermal Expansion - Nonmetallic Solids*, Y.S. Touloukian ed., **IFI/Plenum**, New York, 1977, 173, 392 and 548.
12. *Landolt-Bornstein*, 6 Aufl., II Band, 2 Teil, Springer-Verlag, Berlin, 1962, 1-147 and 1-150.
13. P.C. **CARMAN**: Fluid Flow Through Granular Beds, *Transactions of the Institution of Chemical Engineers*, 15, 1937, 150.
14. S. **ROY** and R.L. **COBLE**, Solubilities of Magnesia, Titania, and Magnesium Titanate in Aluminium Oxide, *Journal of the American Ceramic Society*, 51, 1968, 1.